2011 50th IEEE Conference on Decision and Control and
European Control Conference (CDC-ECC)
Orlando, FL, USA, December 12-15, 2011

Implementation of sEMG-Based Real-Time Embedded Adaptive Finger Force Control for a Prosthetic Hand

Chandrasekhar Potluri, *Member, IEEE*, Madhavi Anugolu, *Member, IEEE*, Yimesker Yihun, Parmod Kumar, Steve Chiu, *Member, IEEE*, Marco P. Schoen, *Senior Member, IEEE*, D. Subbaram Naidu, *Fellow, IEEE*

Abstract—This paper presents surface electromyographic (sEMG)-based, real-time Model Reference Adaptive Control (MRAC) strategy for a prosthetic hand prototype. The proposed design is capable of decoding the prerecorded sEMG signal as well as the sensory force feedback from the sensors to control the force of the prosthetic hand prototype using a PIC 32MX360F512L microcontroller. The input sEMG signal is preprocessed using a Half-Gaussian filter and fed to a fusion based Multiple Input Single Output (MISO) skeletal muscle force model. This MISO system provides the estimated finger forces to be produced as input to the prosthetic hand prototype. A simple MRAC method along with a two stage embedded design is used for the force control of the prosthetic hand. The sensed force at the fingertip is fed back to the controller for real-time operation. The data is transmitted to the computer through an universal asynchronous receiver/transmitter (UART) interface of the proposed embedded design. Results show good performance in controlling the finger force as well as shortcomings of the mechanical design of the prosthetic hand prototype to be addressed in future.

I. INTRODUCTION

In the United States, the number of people with missing limbs because of combat and non-combat operations is over 1.2 million [1]. The number of amputees has substantially increased due to the recent wars in Afghanistan and Iraq. To date, there has been active research to design a prosthetic hand; however, even today, there are no prosthetic devices available at an affordable cost and with tactile or proprioceptive feedback for grasping [2]. In nonindustrial robotics, 'rehabilitation robotics' is an active research area for the last two decades. Rehabilitation robotics is human-centered and addresses a different set of requirements such as mechanical compliance, flexibility, adaptability towards the user, gentleness, safety and, last but not least, humanoid appearance and behavior [3]. Past researches stipulate that human-centered robots must be autonomous with a high level of functionality, pleasure, comfort and ease of use [4]. One interesting domain of rehabilitation robotics is human-machine interface. Human-centered robotics requires a natural means of communication [5], and in the case of electromyographic (EMG) based prosthesis one natural means of interface between the human arm and prosthesis is sEMG itself. The sEMG signals are electrical voltages ranging from -5 to +5 (mV). sEMG signals are always available and their strength and variability depends on different movements and force levels. sEMG signals can be acquired using suitable sensors and can be used as an input to the controller of the hand prosthesis to control the movements and force applied by the fingers. Since, most of the available prostheses employ the users direct vision as a sensory feedback lack in tactile or proprioceptive feedback for grasping [2], and thus half of the upper extremity amputees choose not to use their prosthetic hands on a regular basis [6, 7].The control of a multi-fingered prosthetic hand is difficult as the human hand is a highly complex and nonlinear system with many degrees of freedom [8]. Past research suggests that the typical approach to the control of a prosthetic hand is to use hybrid position and force control [9]. As sEMG signals are collected from the surface of the skin, the signals pass through numerous tissues before they reaches the surface of the skin and are acquired by the sensors [10]. Hence, they are prone to cross-talk, interference and noise. The sEMG is a temporal and spatially modulated signal [11].

Chandrasekhar Potluri is with Measurement and Control Engineering Research Center (MCERC), Idaho State University, Pocatello, Idaho 83201 USA (e-mail: potlchan@isu.edu).

Madhavi Anugolu is with MCERC, Idaho State University, Pocatello, Idaho 83201 USA (email: anugmadh@isu.edu).

Yimesker Yihun is with MCERC, College of Engineering, Idaho State University, Pocatello, Idaho 83201, USA (email: yihuyime@isu.edu).

Parmod Kumar is with MCERC, Idaho State University, Pocatello, Idaho 83201 USA (email: kumaparm@isu.edu).

Steve Chiu is with Department of Electrical Engineering and Computer Science, MCERC, Idaho State University, Pocatello, Idaho 83209 USA (email: chiustev@isu.edu).

Marco P. Schoen is with Department of Mechanical and Nuclear Engineering, MCERC, Idaho State University, Pocatello, Idaho 83209, USA (email: schomarc@isu.edu).

D. Subbaram Naidu is with Department of Electrical Engineering and Computer Science, MCERC, Idaho State University, Pocatello, Idaho 83201 USA (email: naiduds@isu.edu).

978-1-61284-799-3/11/$26.00 ©2011 IEEE

The prediction of skeletal muscle forces corresponding to the sEMG signal is challenging. Usually sEMG measurements are based on single sensor data. For this work we used an array of three sEMG sensors and a force sensing resistor (FSR) to acquire the EMG signal and the corresponding skeletal muscle force. The data from the three sEMG sensors is fused using a fusion algorithm since, the fusion based force shows a better estimation of skeletal muscle force from the corresponding sEMG signal when compared to single sensor data [12]. In order for this design to accomplish its goals, a real-time embedded control system is essential. Such a system combines the hardware and software components to balance the computational, electrical and mechanical workloads across the system. Also the present work utilizes a real-time MRAC which is implemented on an embedded test bed to control the movements and the force of a prosthetic hand prototype with sensory feedback. The input to the real-time control system is a fusion based force estimate. A two stage embedded platform with a simple MRAC strategy is chosen for the force control of the prosthetic hand prototype. The paper is organized as follows. The present section covers the literature review and introduction, and the next section describes the experimental set-up. These are followed by the proposed design, results and discussion, and conclusion and future work.

II. Experimental Set-Up

Fig. 1 shows the experimental set-up used to capture sEMG and force signals. The motor points and the appropriated EMG electrode attachment points of the subject were identified by using a wet probe point muscle stimulator (Rich-Mar Corporation, model number HV 1100.).Here we are using an array of three sensors. The sEMG sensor at the center in Fig. 1 is at the motor point while the other two sensors are adjacent to the motor point. sEMG signals are captured from the surface of the skin using DE 2.1 sEMG sensors with a 16-channel DELSYS® Bagnoli EMG system and LabVIEW™. The sEMG signals are acquired at a sampling rate of 2000 samples per second. Prior to placing the sEMG sensors, the skin surface of the subject was prepared according to the International Society of Electrophysiology and Kinesiology (ISEK) protocols [13].

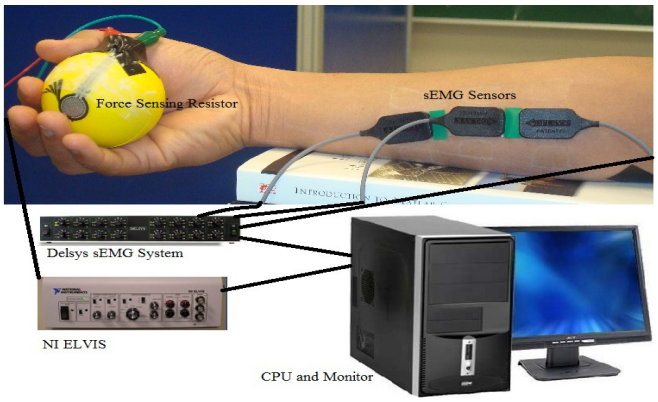

Fig. 1. Experimental Set-Up.

III. Proposed Design

The objective of the embedded system design is for the prosthetic hand fingers to track a force signal as closely as possible. Here, the force signal is inferred from surface EMG (sEMG) signals obtained from the array of the three sEMG sensors located at the arm. The sEMG data is processed by filtering and using a sensor fusion algorithm to facilitate the extraction of the best finger force estimates. Sensor fusion is done in the frequency domain for the sEMG data using a simple elitism based Genetic Algorithm (GA). The data from the three sensors is collected around the corresponding individual motor unit location at the transradial arm location (flexor digitorum superficialis) and before fusing are rectified and filtered using a Half - Gaussian filter, as given by (1).

$$p(EMG|x) = 2 \times \frac{\exp\left(-\frac{EMG^2}{2x^2}\right)}{\sqrt{2\pi x^2}}, \quad (1)$$

where $p(EMG|x)$ is a conditional probability density function, x is a latent driving signal.

System identification (SI) is used to identify the dynamical relationship between the sEMG data from the three sensors u_1, u_2, and u_3 and the corresponding finger force of a healthy male subject. In this fusion algorithm, Output Error (OE) models are used and are constructed for each individual data set. The OE model is given as follows.

$$y(t) = \frac{B(q)}{F(q)}u(t - nk) + e(t), \quad (2)$$

Where B, and $F$are the polynomials, q is shift operator, $e(t)$ is output error, $y(t)$ is system output, u is input, nk is the system delay and t is time index.

Using the three resulting OE models and the fusion algorithm given by [12] a corresponding continuous-time model is constructed as given by the transfer function as

$$G(s) = \frac{B(s)}{F(s)} = \frac{b_{nb}\, s^{(nb-1)} b_{nb-1} s^{(nb-2)} + \cdots + b_1}{s^{nf} + f_{nf}\, s^{nf-1} + \cdots + f_1}, \quad (3)$$

Similar to the discrete-time case nb and nf determine the orders of the numerator and denominator. For multi-input systems, nb and nf are row vectors. b, f are the coefficients of the numerator and denominator polynomials respectively.

A MISO transfer function is constructed based on the poles of three individual OE models corresponding to each sensor. GA is used to find the corresponding zeros. The search area is limited to the unit circle, because a discrete time model is used (and the resulting MISO model is decreased to minimum phase). The number of zeros is at most the number of poles. The number of potential zeros is set to the order of the corresponding denominator. The error squared of the resulting MISO system $H(s)$ (see Appendix)

and the recorded force signal was set as an objective function. The objective function f is constructed as follows,

$$f = \int_{t_0}^{t_f} (\hat{Y}(t) - Y(t)^2 dt = \int_{t_0}^{t_f} \varphi^2(t) dt, \quad (4)$$

where t_0 and t_f are the initial and final time values, $\hat{Y}(t)$ is the fusion model estimated force and $Y(t)$ is the actual force from the FSR.
The MISO system $H(s)$ is constructed as follows,

$$H(s) = \begin{pmatrix} \frac{Z_{1,1}s^n + Z_{1,2}s^{n-1} + \cdots Z_{1,n+1}}{P_{1,1}s^n + P_{1,2}s^{n-1} + \cdots P_{1,n+1}} \\ \frac{Z_{2,1}s^n + Z_{2,2}s^{n-1} + \cdots Z_{2,n+1}}{P_{2,1}s^n + P_{2,2}s^{n-1} + \cdots P_{2,n+1}} \\ \frac{Z_{3,1}s^n + Z_{3,2}s^{n-1} + \cdots Z_{3,n+1}}{P_{3,1}s^n + P_{3,2}s^{n-1} + \cdots P_{3,n+1}} \end{pmatrix}, \quad (5)$$

where $Z's$ and $P's$ are the zeros and poles respectively of the individual transfer function and n is the order of the system.

Feeding the new data sets to the MISO transfer function ($H(s)$) results in an estimated fusion based force $\hat{Y}$.

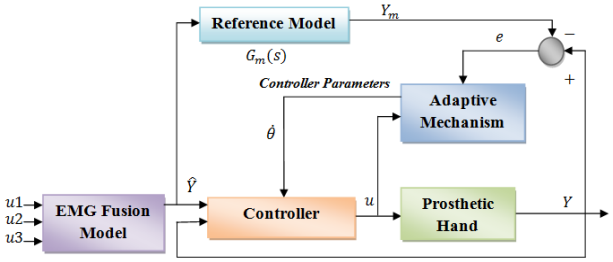

Fig. 2. Block Diagram of Model Reference Adaptive Control (MRAC).

The controller utilized for compensating the dynamics of the prosthetic hand is based on a simple MRAC scheme. During the development of the artificial hand, changes are being undertaken to the mechanical design and drive trains of the hand that affect the dynamics of the finger motion of the prosthesis. In addition, the uncertain characteristics of the kinematic and actuator interaction may lead to different performance than expected. Hence, a simple MRAC controller is devised in order to maintain some performance stability. The controller is given by Fig. 2 where the MIT rule is used for updating the controller parameter θ,

$$\frac{d\theta}{dt} = -\gamma e Y_m \quad . \quad (6)$$

As per the MIT rule [14] the gain parameter γ is selected to achieve the desired performance. In this present work γ is chosen to be 3.0 and the error $e = Y - Y_m$ is computed by the difference of the model reference output Y_m and the true output (force generated by the prosthetic hand). The MRAC is a standard one for which the stability issue has already addressed in literature [14]. Although there are many ways of selecting the reference models (first, second third orders etc.) in this particular case for prosthetic application a first order reference model is chosen to avoid any possible overshoot performance and facilitate fast response time, and is given by

$$G_m(s) = \frac{2}{2s+1} \quad . \quad (7)$$

Implementation:

The force feedback signal is acquired by a Force Sensitive Resistor (FSR). The FSR is mounted on the fingertip of the prosthetic hand prototype as shown in Fig. 3. A simple MRAC is employed to generate the actual force from the FSR, and make it equal to the model reference output in order to impose a desired dynamical response. The proposed control design is implemented on a PIC 32MX360F512L microcontroller in two stages: "Signal Processing" and "Motor Actuation". The Signal Processing stage facilitates the execution and implementation of real-time control strategies. A dsPIC block set is used to generate the C code for the PIC 32 from Simulink®. The dsPIC block set generates a .hex file, and this file is imported in MPLAB® to program the PIC 32.

Signal Processing Stage:

The following modules of the PIC 32 are used for the implementation of the signal processing stage.

a. The Analog Input module
b. The Digital Output module
c. The Output Compare module
d. The UART module

The Analog Input module is used for acquiring the sensory feedback force data from the FSR. The PIC 32 has an internal analog to digital converter (ADC) which has a 10-bit resolution so that it can distinguish up to 1024 different voltage values, usually in the range of 0 to 3.3 volts, and it yields 3mV resolution. The Digital Output module of the PIC 32 is used to generate digital control signals based on the selected control strategy to the motor actuation stage. This module detects the changes in the reference/command signal and flips the direction bits between 0 and 1. The motors switch direction accordingly. Depending on the error, a pulse width modulated (PWM) wave with a specific duty cycle is generated by the Output Compare module. The UART module in the PIC 32 is used to transmit the force data from the microcontroller to the PC via serial communication. In this design, a virtual com port was created to feed the data via USB cable to the computer. MATLAB® is used to read the signals from the ports. This enables the user to troubleshoot and see the performance and accuracy of the designed control strategy.

Motor Actuation Stage:

In this stage, a SN754410 quadruple half-H driver [15] is used to actuate the motor with the corresponding control

signal. The PWM wave from the Output Compare module is connected to the pin1 (1, 2EN) of the H driver. The PWM wave enables this H driver. The speed of the motor depends on the duty cycle of the PWM wave from the Output Compare module which is a function of error $e(t)$. Therefore the speed of the motor is adjusted based on the error to achieve desired performance and accuracy. The digital outputs of the PIC 32 microcontroller are connected to the direction pins of the H driver (pins 2 and 7). Switching the digital outputs to 0 and 1 between the pins makes the motor rotate in clockwise and counter-clockwise directions. This controls the finger to maintain the force levels based on the control strategy. V_{cc1} and V_{cc2} are connected to the 5V supply of the PIC 32 I/O board. This proposed design was tested on an index finger of a prosthetic hand prototype. Fig. 3 shows the test bed for the proposed design. The Mechanical design of the robotic hand prototype is explained in the following section.

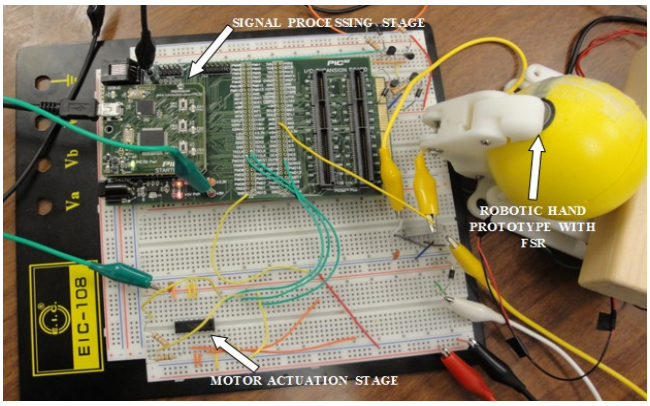

Fig. 3. Embedded Test bed for the proposed design

IV. MECHANICAL STRUCTURE OF THE ROBOTIC HAND PROTOTYPE

The prototype finger has three degrees of freedom actuated by two Pololu 35:1 mini metal gear motors. The main characteristic of this robotic hand is its biologically-inspired parallel actuation system, which is based on the behavior/strength space of the Flexor Digitorum Profundus (FDP) and the Flexor Digitorum Superficialis (FDS) muscles [16]. Fig. 4 depicts the strength space of FDS and FDP muscles. The DC motor in the metacarpal phalange of the finger actuates the Proximal Inter Phalangeal (PIP) joint and through the belt transmission system. It also drives the DIP (Distal Inter Phalangeal) joint. The DC motor at the base of the finger actuates the Meta Carpo Phalangeal (MCP) joint as shown in Fig. 5.

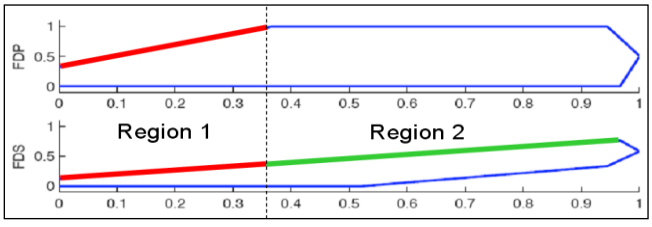

Fig.4. Strength space of FDS and FDP muscles [17]

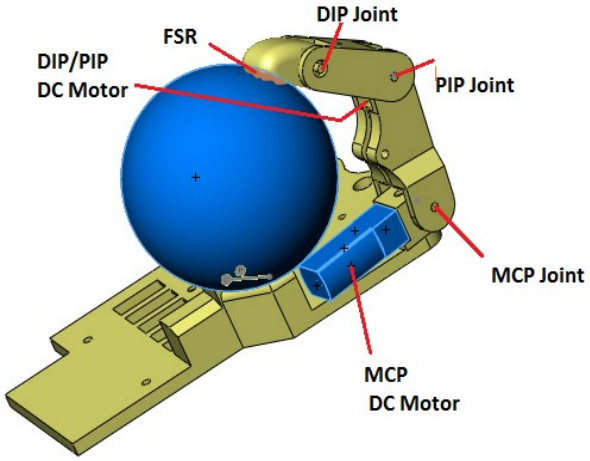

Fig. 5. Actuation scheme for the finger

The DC motors were selected based on their high efficiency (90%) in order to minimize power consumption during more frequently executed tasks (Region 1). An additional criterion is based on the motor's time response, which needs to approximately correspond to the joint speeds of the human hand. Grip force is measured for a number of reasons. For instance, it is typical for real-life gripping scenarios to be recreated to investigate entities such as maximum grip force, and the effects of loading on transmission and range of motions. The requirement to reproduce representative grip conditions means that the force sensor used must not significantly alter the performance characteristics of the grasping action or the operator's ability to use the prosthetic hand prototype. Particularly, in this paper, the Region 1 actuation scheme is considered. In order to sense the normal force applied by the tip of the finger, FSR is attached to the tip of the finger.

V. RESULTS AND DISCUSSION

Data is acquired from the microcontroller through UART channel2 of the PIC 32 micro controller by a virtual com port via USB at 57600 baud rate. The data from the microcontroller is converted into unit16 data type before it is transmitted through the UART. The PIC 32 microcontroller is running at 80 million instructions per second (MIPS) with its phase lock loop (PLL) activated. It is running at an external clock frequency of 8MHz with internal scaling enabled. Fig. 6 depicts the experimental results of the proposed design. The prosthetic hand prototype mathematical model is used instead of the actual hand to obtain the simulation based force output to validate the controller performance. The simulation based force output converges to the fusion model estimate $\hat{Y}$ in approximately 0.9 ms. The simulation based force output exactly matches the fusion model estimated force $\hat{Y}$ after the convergence. The actual force output from the FSR (i.e. Y) closely follows the fusion model estimated force $\hat{Y}$. In Fig. 6 there are some instances where the FSR lost contact with the object, as indicated by a sharp drop in the force curve.

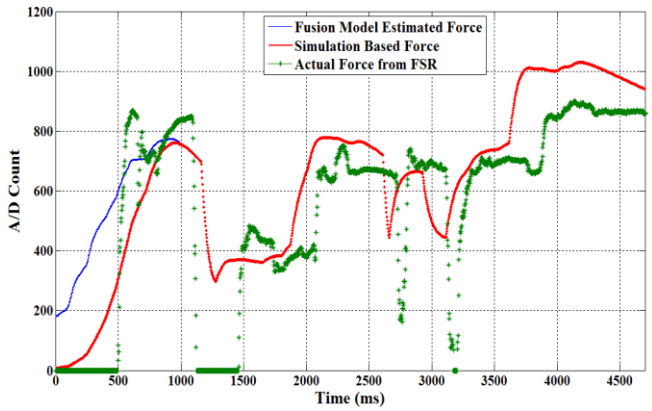

Fig. 6. Fusion based force estimate, simulation based force and actual force from FSR during the grasp.

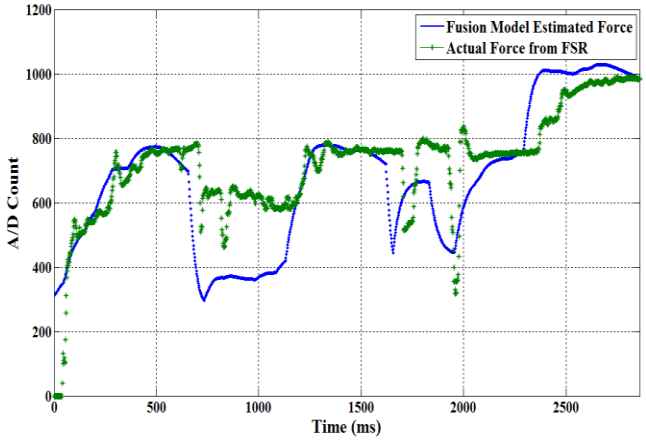

Fig. 7. Fusion based force estimate and actual force from FSR during the grasp (separate experiment).

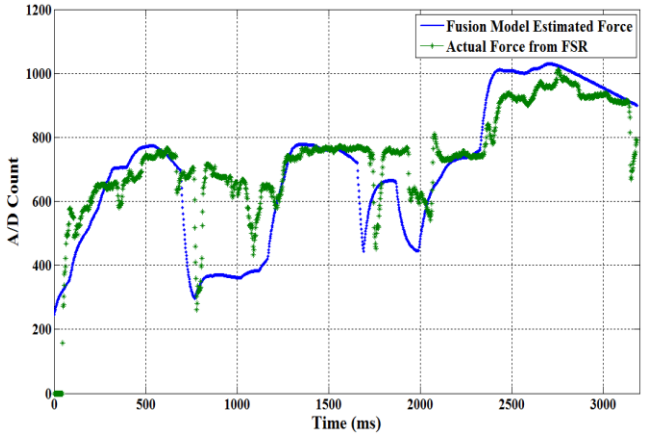

Fig. 8. Fusion based force estimate and actual force from FSR during the grasp (for a repeated experiment).

Fig. 7 shows the fusion model estimated force $\hat{Y}$ and actual force from the FSR (Y) plotted for a separate experiment. In this case, the prosthetic hand prototype is made to maintain a minimum constant force so that the contact between the FSR and the object will not be lost. The same experiment is repeated to test the consistency, and to make sure that the object is in contact with the FSR throughout the experiment.

Fig. 8 shows the repeated experimental results. The proposed control strategy is tracking the force profile and matching the actual force with the model estimated force ($\hat{Y}$). While conducting the experiments, the following observations were made. The DC motors currently employed have the primary task of moving the prosthetic fingers. As the project is ongoing research, the SMA actuation scheme is not yet implemented because of the slow response of the SMA's, and also SMA's have high relaxation time. Therefore it is difficult to track a randomly changing force profile with a slowly responding actuation system. However, as the hand is designed to use the parallel actuation of these DC motors and SMA's, the DC motors alone cannot produce fusion model estimated force. In this work, the DC motors are solely responsible for the motion and force actuation. Since the DC motors have small gear heads, the usual characteristic of gear driver actuation cores occurs: gear backlash. In addition, the DC motors employed were slow in responding to the changes in the force profile. Hence some gaps were observed in the measured force signal. This indicates that there are instances in which the fingertip looses contact due to backlash and vibration problems. However, the profile of the measured force from the FSR has a similar pattern as the fusion model estimated force ($\hat{Y}$). Thus we can conclude that apart from those mechanical transmission problems the implemented control scheme produced promising results. These problems will be considered in a new prototype design that we are currently developing. It is also evident from Figs. 7 and 8 that the minimum constant force is needed to obtain better contact with the object and to accomplish accuracy in tracking the reference force profile. In order to test the precision of the proposed control strategy, 15 different experiments were conducted. The mean of the Pearson's correlation coefficient (see Appendix) for fusion model estimated force ($\hat{Y}$) and the actual force from the FSR (Y) in all the 15 experiments is 0.86. Because of the above mentioned transmission problems and the slow response of the gears, slight variability is observed in the correlation coefficients for the 15 experiments. Hence the difference in tracking the force profile is observed in Figs. 7 and 8. Fig. 9 depicts the validation plot with a different fusion based force estimate $\hat{Y}$ obtained by feeding a different sEMG signal to the MISO transfer function ($H(s)$). The fusion based force estimate, simulation based force and the actual force from the FSR are all shown in Fig. 9. The same mechanical transmission problems and the slow response of gears are observed in this experiment as well. However, the controller is tracking the force profile and the Pearson's correlation coefficients for fusion model estimated force ($\hat{Y}$) and the actual force from the FSR (Y) is 0.84, which is close to other experiments.

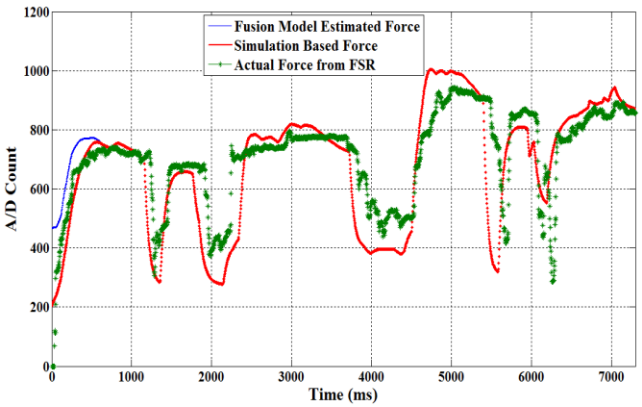

Fig. 9. Validation plot for different model estimated forces.

VI. Conclusion and Future Work

A two-stage real-time embedded MRAC strategy was designed for a prosthetic hand prototype. The proposed design gives good performance when tested on a prosthetic hand prototype, based on tracking a reference force profile. This design facilitates the transmission of the data from the microcontroller to the computer. This design enables the control engineer to increase the accuracy and performance of the design by implementing various novel control strategies and also enables fast trouble shooting.

For the future work, we are planning to implement online model-based force estimation along with controller designs that address the above listed mechanical shortcomings for position and force control, using this embedded platform. It will be interesting to acquire the sEMG signal directly from the arm of a healthy subject transmit to our embedded system instead of using prerecorded sEMG signals, which will be investigated as well in the future. Finally, we plan to use the prototype with five fingers.

Appendix

The resulting MISO transfer function $H(s)$ is constructed as, From u_1 to output,

$$\frac{s^8 - 3.843s^7 + 7.729s^6 - 10.78s^5 + 10.6s^4 - 7.417s^3 + 3.603s^2 - 0.9795s + 0.1192}{s^8 - 4.028s^7 + 6.325s^6 - 4.121s^5 - 1.545s^4 + 5.87s^3 - 5.433s^2 + 2.28s - 0.3496}$$

From u_2 to output,

$$\frac{s^8 - 4.339s^7 + 9.005s^6 - 12.42s^5 + 12.22s^4 - 8.117s^3 + 3.427s^2 - 0.9134s + 0.1424}{s^8 - 4.028\,s^7 + 6.325\,s^6 - 4.121\,s^5 - 1.545\,s^4 + 5.87\,s^3 - 5.433\,s^2 + 2.28\,s - 0.3496}$$

From u_3 to output,

$$\frac{s^8 - 3.522\,s^7 + 6.655\,s^6 - 8.864\,s^5 + 8.183\,s^4 - 5.365\,s^3 + 2.423\,s^2 - 0.557\,s + 0.09585}{s^8 - 4.028\,s^7 + 6.325\,s^6 - 4.121s^5 - 1.545\,s^4 + 5.87\,s^3 - 5.433\,s^2 + 2.28\,s - 0.3496}$$

Pearson correlation coefficient is given by,

$$\rho_{X,Y} = corr(X,Y) = \frac{cov(X,Y)}{\sigma_X \sigma_Y} = \frac{E[(X-\mu_X)(Y-\mu_Y)]}{\sigma_X \sigma_Y}$$

Where X, Y are Random Variables, μ_X and μ_Y are expected values, σ_X, σ_Y are standard deviations respectively. E is expected value operator.

Acknowledgment

This research was sponsored by the US Department of the Army, under the award number W81XWH-10-1-0128 awarded and administered by the U.S. Army Medical Research Acquisition Activity, 820 Chandler Street, Fort Detrick MD 21702-5014. The information does not necessarily reflect the position or the policy of the Government, and no official endorsement should be inferred. For purposes of this article, information includes news releases, articles, manuscripts, brochures, advertisements, still and motion pictures, speeches, trade association proceedings, etc. Further, the technical help from Dr. Alba Perez and Mr. Alex Jensen is greatly appreciated.

References

[1] Amputee Coalition of America (ACA) National Limb Loss Information, Center (NLLIC) Limb Loss Facts in the United States, http://www.amputee-coalition.org, 2005.

[2] D.S. Naidu and C.-H. Chen, "Control Strategies for Smart Prosthetic Hand Technology: An Overview", Book Chapter 14, to appear in a book titled, Distributed Diagnosis and Home Healthcare (D2H2): Volume 2, American Scientific Publishers, CA, January 2011.

[3] Zinn M, Roth B, Khatib O, and Salisbury JK, "A new actuation approach for human friendly robot design," *Int J Robot Res.* 2004; 23(4-5), pp. 379-398.

[4] Bien ZZ, and Stefanov D, "Advances in rehabilitation robotics: Human-friendly technologies on movement assistance and restoration for people with disabilities," *Springer, Berlin (Germany).* 2004.

[5] Heinzmann J, and Zelinsky J, "A safe-control paradigm for human-robot interaction," *J Intell Robot Syst.* 1999; 25(4): pp. 295-310.

[6] D. J. Atkins, D. C. Y. Heard, and W. H. Donovan, "Epidemiologic overview of individuals with upper limb loss and their reported research priorities," *J. Prosthet. Orthot.,* vol. 8, no. 1, p. 2, 1996.

[7] D. H. Silcox, M. D. Rooks, R. R. Vogel, and L. L. Fleming, "Myoelectric prostheses. A long-term follow-up and a study of the use of alternate prostheses," *J. Bone Joint Surg.,* vol. 75, no. 12, pp. 1781–1789, 1993.

[8] T. H. Sueeter, "Control of the Utah/MIT Dextrous hand: Hardware and software hierarchy," *J. Robot. Syst.,* vol. 7, no. 5, pp. 759-790, 1990.

[9] M. H. Raibert and J. J. Craig, "Hybrid position and force control of manipulators," *ASME J. Llyn. Syst. Meas. Contr.,* vol. 102, pp. 126-133, June 1981.

[10] Cram, J.R., Kasman G.S., and Holtz J. *"Introduction to Surface Electromyography,"* Aspen Publisher Inc., Gaithersburg, Maryland, 1998.

[11] Kandel E.R. and Schartz J.H., "*Principles of Neural Science,*" Elsevier/North-Holland, New York, 1981.

[12] Potluri C., Kumar P., Anugolu M., Urfer, A.; Chiu S., Naidu D.S., Schoen, *"Frequency Domain Surface EMG Sensor Fusion for Estimating Finger Forces,"* 32nd Annual International Conference of theIEEE Engineering in Medicine and Biology Society, Buenos Aires, Argentina, August 31 - September 4, 2010.

[13] http://www.isek-online.org/standards_emg.html.

[14] Karl J. Astrom and Bjorn Writtenmark *"Adaptive Control Second Edition",* Dover Publications, Dec 18, 2008.

[15] Texas Instruments "SN754410 quadruple half H-driver data sheet" Dallas, Texas, November 1986 and 1995

[16] Dr. Anthony L. Crawford ,''Design of a Robotic Hand and Simple EMG Input Controller with a Biologically-Inspired Parallel Actuation System for ProstheticApplications''ASME2010,IDETC/CIE 2010

[17] Kutch, J. J., Valero-Cuevas, F. J., "*All muscles are redundant but some are less redundant than others,*" 19th Annual Meeting of the Society for the Neural Control of Movement, Waikoloa Beach, Hawaii, April 2009.